

# An X-ray study of the lower-luminosity LIRGs from GOALS



N. Torres-Albà<sup>1</sup>, K. Iwasawa<sup>1</sup>, D. Sanders<sup>2</sup>, J. Chu<sup>2</sup>, A. Evans<sup>3</sup>,  
J. Mazzarella<sup>4</sup>, T. Díaz-Santos<sup>5</sup>, A. Lee<sup>4</sup>, K. Larson<sup>4</sup>



<sup>1</sup>ICCUB, Universitat de Barcelona, Barcelona; <sup>2</sup>IFA, University of Hawaii, Honolulu, USA; <sup>3</sup>University of Virginia, Charlottesville, USA;

<sup>4</sup>IPAC, Caltech, Pasadena, USA; <sup>5</sup>Universidad Diego Portales, Santiago, Chile

Contact: ntorresalba@icc.ub.edu

## Abstract

We present Chandra observations for a sample of 59 Luminous Infrared Galaxies (LIRGs) from the lower luminosity portion of the Great Observatory All-sky LIRG Survey (GOALS). The GOALS is a multiwavelength study of the most luminous IR-selected galaxies in the local Universe, and this X-ray study, complementing the previous work on the higher-luminosity sample, benefits from the imaging and spectroscopic data from HST, Spitzer and Herschel. With combined X-ray and mid-infrared diagnostics, AGN are found in 33% of the galaxies in the sample, a fraction lower than that found for the higher luminosity sample. The correlation study of far-IR and X-ray emission shows that the GOALS galaxies without traces of AGN appear to be underluminous in X-ray, compared to the previously studied star-forming galaxies with lower star formation rates. Results on X-ray spectral study of the sample will also be presented.

## Introduction

Luminous infrared galaxies (LIRGs) are galaxies with an infrared luminosity between  $10^{11}L_{\odot}$  and  $10^{12}L_{\odot}$ , emitting more in this band than in all other bands combined. Galaxies with infrared luminosity above  $10^{12}L_{\odot}$  are called ULIRGs, Ultra Luminous Infrared Galaxies.

The Great Observatories All-sky LIRG Survey (GOALS, Armus *et al.*, 2009), is combining imaging and spectroscopic data from NASA's Spitzer, Hubble, Chandra and GALEX space-borne observatories in a comprehensive study of over 200 of the most luminous infrared-selected galaxies in the local Universe.

This work directly benefits from Hubble Space Telescope imaging data, used as a visual support for Chandra X-ray contours. Spitzer and Herschel infrared data are used to determine the IR luminosity of the sample's galaxies, as well as determining the contribution to the total output of each galaxy in multiple systems. Spitzer spectroscopy data are also used as a criteria to determine the AGN fraction in the sample.

The objects in GOALS are a complete subset of the IRAS Revised Bright Galaxy Sample (RBGS, Sanders *et al.*, 2003), which contains the brightest 60-micron sources in the extragalactic sky. The LIRGs and ULIRGs targeted in GOALS span the full range of nuclear spectral types (type 1 and 2 AGN, LINERs, and starbursts) and interaction stages (major and minor mergers, and isolated galaxies). They provide an unbiased picture of the processes responsible for enhanced infrared emission in the local Universe, and are excellent analogues for comparisons with infrared and submillimetre selected galaxies at high-redshift.

The sample studied in this work consists of 59 systems from the GOALS sample, 20 of which contain multiple galaxies. It represents the low luminosity part of the GOALS sample, with  $11.05 \leq \log(L_{IR}/L_{\odot}) \leq 11.73$ , incomplete as Chandra data for all systems is unavailable. The redshift range is  $z = 0.003 - 0.037$ .

A complete study of the high luminosity part,  $11.73 \leq \log(L_{IR}/L_{\odot}) \leq 12.57$ , with 44 systems, was carried out by Iwasawa *et al.* (2011), with  $z = 0.010 - 0.088$ .

## AGN selection

From the 79 objects in the sample, 26 show signs from AGN presence either in the infrared spectroscopy, through the presence of the [Ne v]  $14.2 \mu\text{m}$  line; or in X-rays. This represents a 33% of our sample, lower than the 50% found for the high luminosity sample in Iwasawa *et al.* (2011).

Galaxies with a hardness ratio higher than -0.3 (defined as  $HR = (H - S)/(H + S)$ , where  $H$  and  $S$  are the background-corrected counts in the 2–8 keV and 0.5–2 keV bands, respectively), presence of the 6.4 keV Fe K line and/or absorbed AGN features, are classified as AGN.

No.	Name	VO	YKS	D <sub>agn</sub>	[Ne v]	6.2 $\mu\text{m}$ EQW	X-ray (CLA)
(1)	(2)	(3)	(4)	(5)	(6)	(7)	(8)
45	UGC 08387	L	cp	0.5	Y	N	N
57	F06076-2139(S)	-	-	-	N	N	C
64	III Zw 035 (S)	L	S2	0.7	N	-	C
67	F16399-0937(S)	-	cp	0.2	N	N	C
68	16164-0746	L	S2	0.7	Y	N	C
71	NGC 2623	-	-	-	Y	N	C
72	IC 5298	-	-	-	Y	N	A
79	NGC 5256 (NE)	S2	S2	0.7	Y(u)	N	A
79	NGC 5256 (SW)	L	cp	0.6	Y(u)	N	N
85	F17138-1017	-	-	-	N	N	C
100	NGC 7130	L	S2	0.9	Y	N	L
105	NGC 7592 (E)	H	H	0	Y(u)	N	N
105	NGC 7592 (W)	S2	S2	0.7	Y(u)	N	N
107	NGC 4922 (N)	L(u)	S2(u)	0.6(u)	Y	N	A
114	NGC 0232	H	cp	0.4	Y	N	N
120	CGCG 049-057	-	-	-	N	N	C
121	NGC 1068	S2	S2	1	Y	-	L
127	MCG-03-34-064	-	H	0	Y	Y	AL
136	MCG-01-60-022	-	-	-	N	-	CA
142	NGC 5135	-	S2	0.8	Y	N	LA
144	IC 0860	-	-	-	N	N	C
169	ESO 343-IG13 (N)	H	cp	0.2	N	N	C
191	ESO 420-G13	-	H	0.4	Y	N	N
194	ESO 432-IG6 (NE)	-	-	-	N	N	A
194	ESO 432-IG6 (SW)	-	-	-	N	N	A
198	NGC 1365	-	-	-	N	N	CLA

**Table 1** : Table of AGN diagnostics. (1) Number of the object as in Armus *et al.* (2009). (2) Galaxy name. (3) Optical class as in Veilleux *et al.* (1999). (4) Optical class from Yuan *et al.* (2010). (5) AGN fraction, see Yuan *et al.* (2010) for details. (6) Detection of [Ne v]  $14.2 \mu\text{m}$  from Petric *et al.* (2011). (7) X-ray evidence of AGN presence through Chandra spectrum analysis; C: X-ray colour ( $HR \geq -0.3$ ), L: 6.4 keV Fe K line, A: absorbed AGN feature. (u) stands for "unresolved" in a double system.

## Spectral study

Here we present typical X-ray spectra for a starburst galaxy, NGC 3256, which doesn't trigger any of the X-ray AGN selection criteria. MCG-03-34-064, on the other hand, is classified as an AGN through two of the X-ray criteria (iron line and a high increase of X-ray flux at higher energies, which is an absorbed AGN feature).

NGC 5135 presents a high energy excess, which can be fitted as an iron line at 6.41 keV. It is interpreted as marginal evidence for AGN presence, due to the limited amount of counts detected by Chandra at high energies.

All the presented spectra have been corrected for detector response and converted into flux density units.

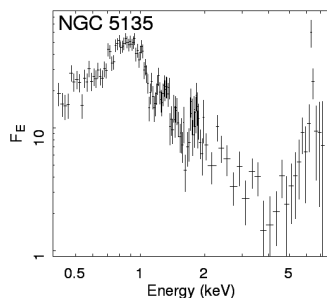
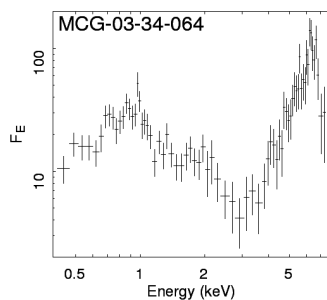
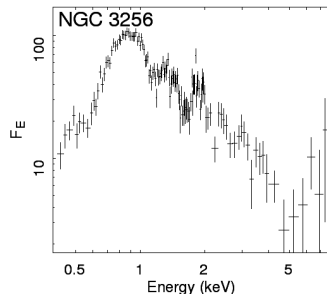


**Figure 1** : Chandra X-ray spectrum of the starburst galaxy NGC 3256, the absorbed AGN MCG-03-34-064 and NGC 5135, for which there is marginal evidence of AGN.

## Chandra contours on optical images

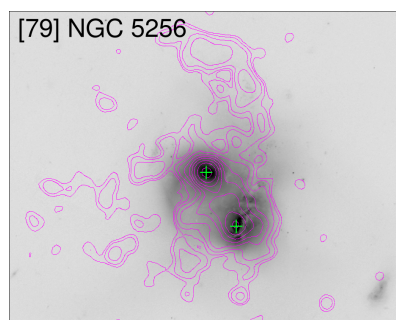


**Figure 2** : Chandra 0.5-7 keV contours (pink) on HST I band image for NGC 5256. Hard band (2-7 keV) X-ray peaks are marked with a green cross.

## Correlation between IR and X-ray emission in LIRGs

In astronomy, many methods are used to estimate the star formation rate in galaxies, the basis of which is quantifying the amount of hot, young and short-lived stars. One of these methods is a measurement of the energy deposited in the dust of the interstellar medium by these stars, which is obtained through far-infrared luminosity measurements. Therefore, far-infrared luminosity can be directly related to the star formation rate.

In galaxies with a considerable amount of star formation, such as starburst galaxies, emission in other wavelengths can be somewhat related to young and massive stars, such as X-ray luminosity (e.g. X-ray binaries emission, supernova remnants (SNRs)). Therefore, it has been suggested that if a good correlation between X-ray luminosity and IR luminosity exists in galaxies, the star formation rate (SFR) can be directly inferred from the X-ray luminosity (e.g. Ranalli *et al.*, 2003; Grimm *et al.*, 2003; Mineo *et al.*, 2014). However, the applicability of this method has been questioned due to experimental results at higher SFRs (e.g. Iwasawa *et al.*, 2009).

In Figure 3, X-ray luminosity is plotted as a function of infrared luminosity. Galaxies classified as AGN (see this work's Table 1 and Table 5 from Iwasawa *et al.* (2011)) have been removed.

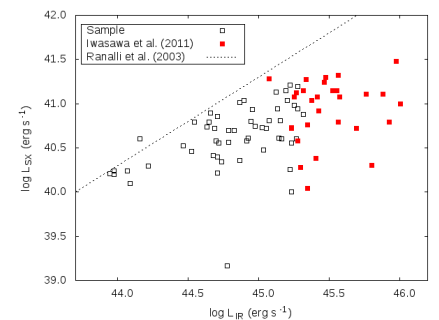
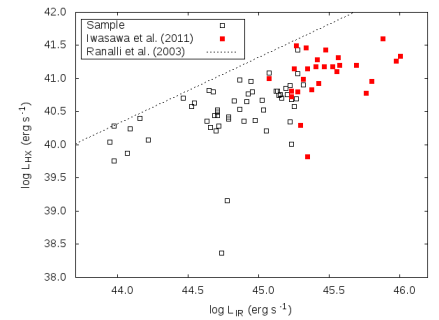


**Figure 3** : X-ray luminosity in soft band (top) and hard band (bottom) versus the infrared luminosity (calculated as in Ranalli *et al.* 2003), for both the galaxies in the present sample and the galaxies in the high luminosity sample (Iwasawa *et al.* (2011)). The line shows the correlation derived by Ranalli *et al.* 2003 for galaxies at lower infrared luminosities.

As seen in Figure 3, LIRGs and ULIRGs deviate from the correlation found at lower luminosities, and appear to be underluminous in X-rays, with this trend increasing as infrared luminosity increases.

## References

- Armus, L., Mazzarella, J., Evans, A., *et al.* 2009, PASP, 121, 559A
- Grimm, H.-J., Gilfanov, M. & Sunyaev, R. 2003, MNRAS, 339, 793G
- Iwasawa, K., Sanders, D.B., Evans, A.S., *et al.* 2009, ApJ, 695L, 1031
- Iwasawa, K., Sanders, D.B., Teng, S.H., *et al.* 2011, A&A, 529A, 1061
- Mineo, S., Gilfanov, M., Lehmer, B.D., *et al.* 2014, MNRAS, 437, 1698M
- Petric, A.O., Armus, L., Howell, J., *et al.* 2011, ApJ, 730, 28P
- Ranalli, P., Comastri, A. & Setti, G. 2003, A&A, 399, 39R
- Sanders, D.B., Mazzarella, J.M., Kim, D.-C., *et al.* 2003, AJ, 126, 1607S
- Veilleux, S., Kim, D.-C. & Sanders, D.B. 1999, ApJ, 522, 113V
- Yuan, T.-T., Kewley, L.J. & Sanders, D.B. 1999, ApJ, 709, 884Y